Molecular Dynamics of Monopyrenyl Lipids in Liposomes from Global Analysis of Time-Resolved Fluorescence of Pyrene Monomer and Excimer Emission†

E. G. Novikov,§ N. V. Visser,‡ V. G. Malevitskaia,§ J. W. Borst,‡ A. van Hoek,‡ and A. J. W. G. Visser*,‡

Laboratory of Biochemistry, Department of Biomolecular Sciences, MicroSpectroscopy Centre, Wageningen University, Dreijenlaan 3, 6703 HA Wageningen, The Netherlands, and Systems Analysis Department, Belarussian State University, F. Skariny Avenue 4, Minsk 220050, Belarus

Received April 1, 2000. In Final Form: June 26, 2000

The diffusion coefficients of 1-palmitoyl-2-(pyrenodecanoyl)-*sn*-glycero-3-phosphocholine ($pyr_{10}PC$) in different bilayer membranes are determined from global analysis of the time-resolved fluorescence of the pyrene monomer and excimer emissions. The global kinetic model involves a time-dependent reaction rate coefficient derived from the analytical solution of the diffusion equation for bimolecular reactions in the two-dimensional surface of the membrane. The bilayer membranes are single unilamellar vesicles (SUV's or liposomes) composed of dioleoylphosphatidylcholine (DOPC), 1-stearoyl-2-arachidonoylphosphatidylcholine (SAPC), or dipalmitoylphosphatidylcholine (DPPC). All SUV's except the one composed of DPPC are in the liquid crystalline state. Liposomes composed of mixtures of DOPC and SAPC in various molar ratios are also investigated by the pyrene excimer reaction. The diffusion constant becomes larger when the fraction of SAPC in the mixed bilayers increases, indicating an apparent increase in fluidity. The latter observation is supported by photostationary measurements of the pyrene excimer to monomer intensity ratios of the same liposomes.

Introduction

Pyrene-containing phospholipids can report on their lateral mobilities in bilayer membranes because of their ability to form excimers when pyrene molecules in the excited state collide with others in the ground state.[1] The excimer fluorescence is at longer wavelengths than the monomer fluorescence. The ratio of excimer to monomer emission intensities (*E*/*M*) is a measure of the rate of excimer formation, which is determined by the frequency of collisions between pyrene moieties and hence can be related to parameters describing membrane dynamics and organization (for reviews, see refs 2 and 3). In short, *E*/*M* is indicative of the fluidity: the larger this ratio, the more fluid the membrane (in a strict sense "microfluidity" is a better definition, since the dynamic properties of the local probe environment are investigated). The dynamic processes governing the excimer formation have been modeled with a lattice model, which considers lipid probes migrating in a trigonal lattice of lipids by exchanging positions with one of their six neighbors.[4,5] In addition to measuring steady-state *E*/*M* ratios, time-resolved fluorescence techniques can be utilized to determine diffusion coefficients of pyrene-containing lipids in membranes using a model of diffusion-controlled bimolecular reactions in two dimensions derived in the mid-1970s by Razi Naqvi.[6] Validation of the latter model in the case of long-range diffusion was accomplished using time-resolved fluorescence applied to monopyrenylphosphatidylcholine (abbreviated as $pyr_{10}PC$; 1-palmitoyl-2-(pyrenodecanoyl)-*sn*-glycero-3-phosphocholine) in 1-palmitoyl-2-oleoylphosphatidylcholine (POPC) vesicles.[7] The collision between two $pyr_{10}PC$'s is an intermolecular event and reports on lateral diffusion of this probe lipid dispersed in liposomes.

In this study, we have determined lateral diffusion coefficients of $pyr_{10}PC$ in different liposomes using time-resolved fluorescence methods. One membrane system consisted of liposomes composed of dioleoylphosphatidylcholine (DOPC, which is a symmetrically substituted phosphatidylcholine with one double bond in each chain), 1-stearoyl-2-arachidonoylphosphatidylcholine (SAPC, which is a mixed-chain phosphatidylcholine with a saturated *sn*-1 chain and four double bonds in the *sn*-2 chain), or fractional mixtures of DOPC and SAPC. These liposomes are fluid membranes, and we were interested in investigating the effect of membrane curvature on the lateral diffusion of incorporated $pyr_{10}PC$. The arachidonyl chain having four unsaturated bonds does not form an extended linear chain but is folded back almost halfway along the fatty acid. Liposomes in the gel phase were prepared from dipalmitoylphosphatidylcholine (DPPC). Although we realize that the excimer formation of pyrene lipids in membrane bilayers is diffusion controlled only above the phase transition temperature,[2] it was decided to subject the results of these experiments to a decay

* Corresponding author. Tel: +31-317-482862. Fax: +31-317-484801. E-mail: ton.visser@laser.bc.wau.nl.

† Part of the Special Issue "Colloid Science Matured, Four Colloid Scientists Turn 60 at the Millennium". Dedicated to Professor Josef Holzwarth on the occasion of his 60th birthday.

‡ Wageningen University.

§ Belarussian State University.

(1) Förster, T.; Kasper, K. *Z. Elektochem.* **1955**, *59*, 976−980.

(2) Galla, H.-J.; Sackmann, E. *Biochim. Biophys. Acta* **1974**, *339*, 103−115.

(3) Visser, A. J. W. G. *Curr. Opin. Colloid Interface Sci.* **1997**, *2*, 27−36.

(4) Eisinger, J.; Flores, J.; Petersen, W. P. *Biophys. J.* **1986**, *57*, 987−1001.

(5) Sassaroli, M.; Vauhkonen, M.; Perry, D.; Eisinger, J. *Biophys. J.* **1990**, *49*, 281−290.

(6) Razi Naqvi, K. *Chem. Phys. Lett.* **1974**, *28*, 280−284.

(7) Martins, J.; Vaz, W. L.; Melo, E. *J. Phys. Chem.* **1996**, *100*, 1889−1895.

10.1021/la000512r CCC: $19.00
Published on Web 09/15/2000

analysis to verify at least that the lateral diffusion is an order of magnitude slower than that in fluid membranes.

Also investigated in this paper is the parametric modeling of the fluorescence kinetics of monomer and excimer emissions of $pyr_{10}PC$. We have extended the approach developed in ref 7 by global analysis of both monomer and excimer emission decays, thereby linking the common parameters. As the model developed by Razi Naqvi[6] contains a number of parameters that are highly correlated, we have critically assessed physically meaningful values of the different parameters involved.

Experimental Section

Chemicals. Dioleoylphosphatidylcholine (DOPC), 1-stearoyl-2-arachidonoylphosphatidylcholine (SAPC), and dipalmitoylphosphatidylcholine (DPPC) were purchased from Sigma (Zwijndrecht, The Netherlands), and 1-palmitoyl-2-(pyrenodecanoyl)-*sn*-glycero-3-phosphocholine ($pyr_{10}PC$) was obtained from Molecular Probes (Leiden, The Netherlands).

Vesicle Preparation. Unilamellar membrane vesicles containing desired fractions of pyrene-labeled phospholipids were prepared by injecting not more than 10 μL samples of phospholipid ethanol solutions (the total lipid concentration was always 50 μM at each desired probe:lipid mole fraction) through a Hamilton syringe into 1 mL portions of a magnetically stirred buffer solution (PBS) at temperatures at least 15 deg higher than the transition temperatures of the chosen liposomes. With fluorescence correlation spectroscopy, it was shown that the average size of these vesicles was ca. 25 nm.[8]

Steady-State Fluorescence Measurements. Fluorescence spectra were obtained with a Spex Fluorolog 3.2.2 spectrofluorometer equipped with a thermostated cuvette holder for quartz cuvettes (Hellma, 1 cm path length). The temperature was 20 °C, and the slit widths used were 0.5 nm for excitation and 1.0 nm for emission.

Time-Resolved Fluorescence Measurements. Time-resolved fluorescence measurements were carried out using the time-correlated single-photon-counting technique (for detailed description see ref 9). A frequency-doubled, synchronously pumped, cavity-dumped dye laser (DCM) was used for excitation. The repetition rate of excitation pulses was 476 kHz, the wavelength 343 nm, the pulse duration around 4 ps, and the pulse energy in the tenths of 1 pJ range. Quartz cuvettes (Hellma, 1 cm path length) were mounted in a thermostated cell holder, and the temperature of the experiments was 20 °C. Emission light was collected through a polarizer at the magic angle with a single-photon-counting detection system. A combination of filters (a Schott KV 370 cutoff filter combined with a Schott 374.6 or 470.0 nm line filter) was used to select the desired emission wavelength. After the emission of the sample was measured, the background emission of a corresponding sample without the pyrene lipid was measured and used for background subtraction. To obtain a dynamic instrumental response as a reference for deconvolution, a reference compound (1,4-bis(5-phenyl-2-oxazolyl)benzene (POPOP) in ethanol) characterized by a single-exponential fluorescence decay time of 1.35 ns[10] was used (for further details see the Data Analysis section).

Data Analysis

Models. The models for monomer and excimer emissions are based on the general representation in Scheme 1. The monomer M*, being excited by an infinitely narrow optical pulse $\delta(t)$, can undergo a reaction in the excited state with an unexcited monomer M, thus forming the (excited) excimer E*. The time-dependent rate of this reaction is denoted by $k(t)$. Excited monomers and excimers can relax to the ground state, emitting light with rate

Scheme 1. General Representation of the Pyrene Excimer Reaction

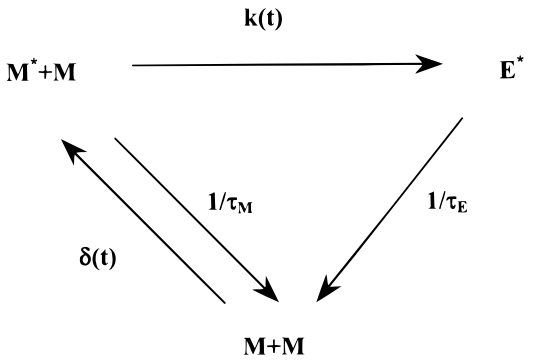

constants $1/\tau_M$ and $1/\tau_E$, respectively. While relaxing to the ground state, an excimer is dissociated into two monomers.

The monomer fluorescence intensity decay excited by an infinitely narrow optical pulse is given by[11,12]

$$I_M(t) = I_M \exp[-t/\tau_M - \int_0^t k(x)\,dx] \quad (1)$$

where I_M is the fluorescence intensity at zero time ($t = 0$), τ_M is the monomer fluorescence decay time, and $k(x)$ is the time-dependent reaction rate coefficient, derived from the analytical solution of the diffusion equation,[13] subject to Collins and Kimball boundary conditions and uniform initial conditions,[6] i.e.

$$k(x) = (16Dh^2c/\pi)\int_0^\infty \exp(-2Dxu^2/R^2)/\{u[(hJ_0(u) + uJ_1(u))^2 + (hY_0(u) + uY_1(u))^2]\}\,du \quad (2)$$

where $h = \alpha R/D$, J_ν and Y_ν are Bessel functions of the first and second kinds, respectively, of order ν ($\nu = 0, 1$), c is the concentration of the excimer probe (molecules per area), D is the diffusion coefficient of one reactant, R is the reaction distance, and α is the intrinsic reaction rate constant. When $\alpha \to \infty$, reaction always occurs at contact, and when $\alpha \to 0$, reaction never occurs.[11] The excimer fluorescence intensity decay is represented by a convolution of the monomer decay and its own monoexponential excimer decay law:[11,14]

$$I_E(t) = k(t)\, I_M(t) \otimes \exp(-t/\tau_E) \quad (3)$$

where $\otimes$ denotes convolution and τ_E is the fluorescence decay time of the excimer.

Analysis. To avoid the distortions related to the wavelength dependence of the detecting path, analysis was performed by the reference reconvolution method,[10] where the observed detected decay is represented via the monoexponential decay of a reference compound that emits at the same wavelength as the investigated samples (POPOP in this case). Applying the reference reconvolution method to the analysis of monomer and excimer fluorescence decays leads to

$$F_M(t) = F_R(t) \otimes [I_M'(t) + I_M(t)/\tau_R] + F_R(t)\, I_M(0) \quad (4)$$

$$F_E(t) = F_R(t) \otimes [I_E'(t) + I_E(t)/\tau_R] + F_R(t)\, I_E(0) \quad (5)$$

where $F_R(t)$ and τ_R are the fluorescence decay function and decay time of the reference, respectively, and $I_M'(t)$ and $I_E'(t)$ are the first-order time derivatives of monomer and excimer decay laws, respectively. The amplitudes at zero time can be derived directly from eqs 1 and 3 as

(8) Hink, M.; Visser, A. J. W. G. In *Applied Fluorescence in Chemistry, Biology and Medicine*; Rettig, W., Strehmel, B., Schrader, S., Seifert, H., Eds.; Springer-Verlag: Berlin, 1998.

(9) Pap, E. H. W.; Hanicak, A.; van Hoek, A.; Wirtz, K. W. A.; Visser, A. J. W. G. *Biochemistry* **1995**, *34*, 9118−9125.

(10) Vos, K.; van Hoek, A.; Visser, A. J. W. G. *Eur. J. Biochem.* **1987**, *165*, 55−63.

(11) Szabo, A. *J. Phys. Chem.* **1989**, *93*, 6929−6939.

(12) Hauser, M.; Wagenblast, G. In *Time-Resolved Fluorescence Spectroscopy in Biochemistry and Biology*; Cundall, R. B., Dale, R. E., Eds.; Plenum Press: New York, 1983.

(13) Carslaw, H. S.; Jaeger, J. C. *Conduction of Heat in Solids*; Oxford University Press: New York, 1959.

(14) Berberan-Santos, M. N.; Martinho J. M. G. *Chem. Phys.* **1992**, *164*, 259−269.

$$I_M(0) = I_M, \quad I_E(0) = 0 \tag{6}$$

After combination of eqs 1, 4, and 6, the detected decay for the monomer via the fluorescence decay of the reference compound is obtained:

$$F_M(t) = F_R(t) \otimes [(1/\tau_R - 1/\tau_M - k(t))I_M(t)] + I_M F_R(t) \tag{7}$$

From eqs 3, 5, and 6, the detected excimer fluorescence profile is obtained as

$$F_E(t) = F_R(t) \otimes [(1/\tau_R - 1/\tau_E)I_E(t) + k(t)\, I_M(t)] \tag{8}$$

The fit of the monomer and excimer fluorescence decay parameters was based on the Marquardt nonlinear method of least squares, described in detail elsewhere.[15] Since the time-dependent reaction rate coefficient $k(t)$ is equally present in the models for monomer (eq 1) and excimer (eq 3) emissions, the parameters characterizing $k(t)$ (i.e., concentration c, diffusion coefficient D, and the intrinsic reaction rate constant α) are the same for both decays. This implies the necessity of a global parametric fit of the fluorescence decay curves for monomer (eq 7) and excimer (eq 8) emissions, assuming that the common parameters are equal for both curves. The reaction radius R was fixed to a value of 7.1 Å, obtained from refs 7 and 16 for two pyrene molecules. The goodness of fit was judged by χ^2 criteria, visual inspection of the residuals between experimental and fitted curves and the autocorrelation function of residuals. The error estimation of the recovered parameters was performed by the exhaustive search method.[17]

Results and Discussion

Fluorescence Spectra. Figure 1 shows the fluorescence spectra of $pyr_{10}PC$ in (A) SAPC, (B) DOPC, and (C) DPPC membranes at a low probe:lipid molar ratio (1:1000) and a higher probe:lipid molar ratio (1:150). At these probe concentrations, no influence of the probe molecules on the liposomal system is expected.[7] Clearly, at the low probe:lipid molar ratio, hardly any excimer emission is observed, whereas, at the higher probe:lipid molar ratio, a distinct excimer emission spectrum becomes visible.

The pyrene monomer fluorescence spectrum exhibits significant fine structure in the form of five predominant peaks (see Figure 1A). Peak 3 (I_3, at longer wavelength) shows minimal intensity variation with polarity, whereas peak 1 (I_1, at shorter wavelength) shows significant intensity enhancement when the environment is more polar. Thus, the intensity ratio I_3/I_1 is an empiric measure of polarity: the larger I_3/I_1, the larger the apolarity in the vicinity of the pyrene probe.[18−20] The I_3/I_1 values for all lipid bilayers are collected in Table 1. It appears that the unsaturated liposomes exhibit a higher apolarity than saturated liposomes. Such a behavior is also observed for a DODAB-pyrene probe in DODAB vesicles when the membrane passes the phase transition: above the phase transition temperature, the DODAB bilayer membrane becomes more apolar.[21]

The E/M ratios for $pyr_{10}PC$ in DOPC and SAPC vesicles are different (E/M ratios for $pyr_{10}PC$ in all lipid bilayers are collected in Table 1). At 20 °C, both membranes are far above the phase transition temperatures (−20 and −13 °C, respectively[22]), and the immediate conclusion is that the fluidity in the SAPC bilayer midplane is larger, considering that the position of the pyrene moiety of the phospholipid is 17 Å from the headgroups.[23] It can also be noticed that the E/M ratio gradually increases with an increasing molar fraction of SAPC in the mixture. The latter observation indicates that all phospholipid constituents are homogeneously dispersed in the liposome.

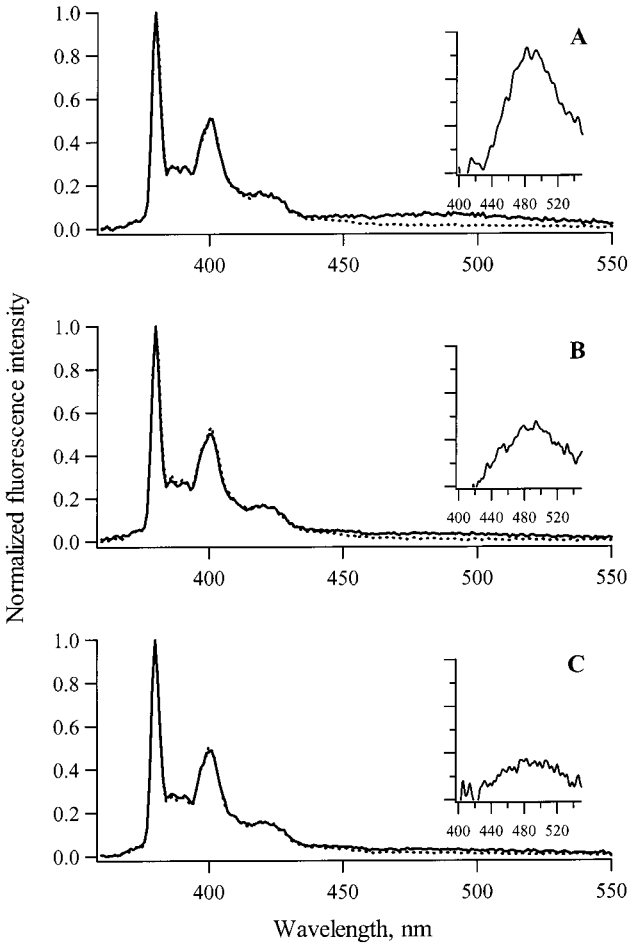

Figure 1. Fluorescence emission spectra of $pyr_{10}PC$ in different liposomes: (A) SAPC; (B) DOPC; (C) DPPC. The [$pyr_{10}PC$]:[phospholipid] ratios were 1:1000 (broken lines) and 1:150 (solid lines). The insets give the enlarged difference spectra representing excimer emissions.

Table 1. Pyrene I_3/I_1 and E/M Ratios for a Pyrene Lipid in Different Membrane Environments[a]

sample	I_3/I_1	E/M	sample	I_3/I_1	E/M
100% DOPC	0.290	0.036	100% SAPC	0.292	0.074
25% SAPC, 75% DOPC	nd	0.049	100% DPPC	0.271	0.030
50% SAPC, 50% DOPC	nd	0.057			

[a] I_3/I_1 was only determined for the pure membrane systems at a [probe lipid]:[phospholipid] ratio of 1:1000. E/M was determined for all membrane systems at a [probe lipid]:[phospholipid] ratio of 1:150. I_1 is the fluorescence intensity at 380 nm; I_3 is the fluorescence intensity at 391 nm; M ($=I_M$) is the fluorescence intensity at 380 nm; E ($=I_E$) is the fluorescence intensity at 480 nm.

Time-Resolved Fluorescence Decay. In Figure 2A, the experimental decays of the monomer fluorescence of

(15) Bevington, P. R. *Data Reduction and Error Analysis for the Physical Sciences*; McGraw-Hill: New York, 1969.
(16) Edward, J. T. *J. Chem. Educ.* **1970**, *47*, 261−270.
(17) Beechem, J. M.; Gratton, E.; Ameloot, M.; Knutson, J. R.; Brand, L. In *Topics in Fluorescence Spectroscopy*; Lakowicz, J. R., Ed.; Plenum Press: New York, 1991; Vol. 2.
(18) Kalyanasundaram, K.; Thomas, J. K. *J. Am. Chem. Soc.* **1977**, *99*, 2039−2044.
(19) Komatsu, H.; Rowe, E. S. *Biochemistry* **1991**, *30*, 2463−2470.
(20) Nascimento, D. B.; Rapuano, R.; Lessa, M. M.; Carmona-Ribeiro, A. M. *Langmuir* **1998**, *14*, 7387−7391.
(21) Jung, M.; Hubert, D. H. W.; van Veldhoven, E.; Frederik, P. M.; Blandamer, M. J.; Briggs, B.; Visser, A. J. W. G.; van Herk, A. M.; German, A. L. *Langmuir* **2000**, *16*, 968−979.
(22) Koynova, R.; Caffrey, M. *Biochim. Biophys. Acta* **1998**, *1376*, 91−145.
(23) Sassaroli, M.; Ruonala, M.; Virtanen, J.; Vauhkonen, M.; Somerharju, P. *Biochemistry* **1995**, *34*, 8843−8851.

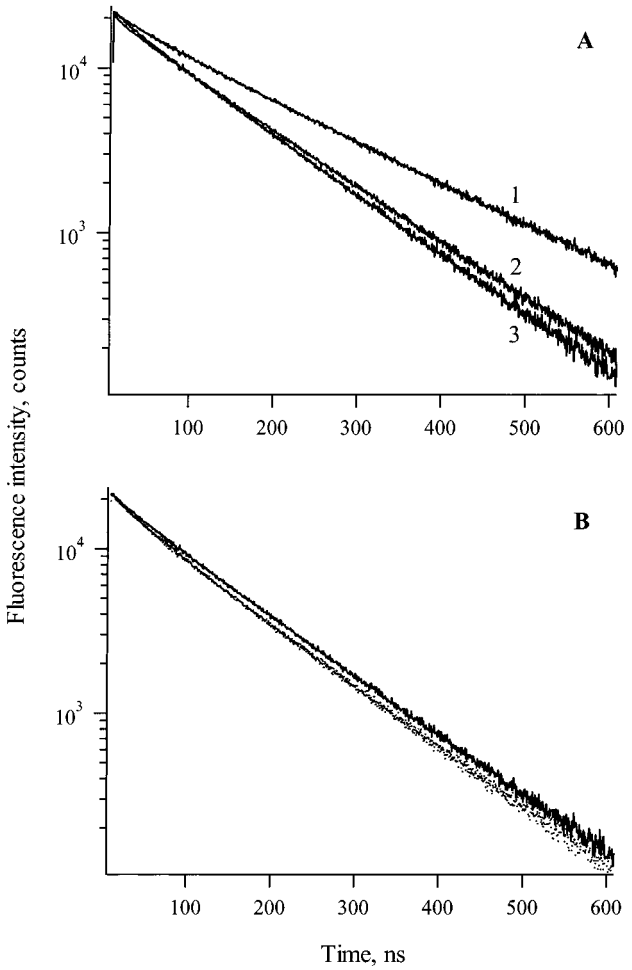

Figure 2. Fluorescence decay curves for monomer emissions of $pyr_{10}PC$ in different liposomes. The decay curves are normalized for convenience. Panel A: The [$pyr_{10}PC$]:[phospholipid] ratio was 1:1000 for DPPC membranes (curve 1), DOPC membranes (curve 2), and SAPC membranes (curve 3). Panel B: Two decays are shown for $pyr_{10}PC$ in SAPC liposomes. The slower decay is for a probe:phospholipid molar ratio of 1:1000, and the faster decay, for a ratio of 1:150.

$pyr_{10}PC$ in liposomes consisting of DPPC (curve 1), DOPC (curve 2), and SAPC (curve 3) are displayed. The [probe]:[lipid] ratio is 1:1000 in all cases, and excimer emission is hardly detectable. The fluorescence decay is clearly slowest when the $pyr_{10}PC$ is in membranes in the gel phase and faster when the probe lipid is dispersed in fluid membranes. The decay appears to be faster for $pyr_{10}PC$ in SAPC as compared to DOPC. An example of the effect of increasing [probe]:[lipid] ratio on the monomer fluorescence decay is presented in Figure 2B for $pyr_{10}PC$ in SAPC. For a [probe]:[lipid] concentration ratio of 1:150, the decay is more rapid, since the probability of forming excimers has increased, resulting in an additional decay channel for excited monomers.

Time-Resolved Fluorescence Decay Analysis. In the analysis, fluorescence kinetics of monomer and excimer emissions of four samples with different combinations of the unsaturated phospholipids SAPC and DOPC were combined into one set and simultaneously fitted. This led to a global analysis configuration containing eight time-dependent fluorescence profiles: monomer and excimer emissions for each of four samples. As stated under Data Analysis, parameters such as the concentration, diffusion coefficient, and intrinsic reaction rate constant must always be the same for the monomer and excimer emissions of one membrane sample and therefore must be kept equal in the fitting procedure. In a first approximation, it was assumed that the concentration and intrinsic reaction rate constant were the same for the four membrane preparations in the set and these parameters were also linked in the fitting procedure. The link of these parameters allowed us to obtain a clear dependence of the translation diffusion coefficients on composition in SUV's made from different fractional mixtures of SAPC and DOPC, undistorted by the possible fluctuations in the estimates of concentrations or intrinsic reaction rate constants. The parameters that were not linked are the monomer and excimer decay times, since they may reflect kinetically different processes deactivating the excited state which cannot be resolved, and, of course, scaling factors for monomer and excimer emission intensities.

Table 2. Dependence of the Diffusion Coefficient *D* and Decay Times of Monomer (τ_M) and Excimer (τ_E) on the Molar Percentage of SAPC in Mixed DOPC/SAPC Liposomes[a]

sample	$10^{-8}D$, $cm^2\ s^{-1}$	τ_M, ns	τ_E, ns
100% DOPC	7.2	165	63
	[6.6; 9.1]	[152; 173]	[58; 65]
25% SAPC, 75% DOPC	9.6	165	62
	[7.6; 10.6]	[151; 173]	[57; 65]
50% SAPC, 50% DOPC	10.5	163	53
	[9.1; 12.7]	[150; 171]	[50; 57]
100% SAPC	16.1	174	55
	[13.4; 18.9]	[161; 182]	[52; 59]

[a] Confidence intervals are given at the 67% level.

The parameters recovered after global analysis are collected in Table 2. Typical examples of experimental and fitted decay curves are presented in Figure 3 (for $pyr_{10}PC$ in a DOPC/SAPC liposome mixture at a 1:1 molar ratio). The fitted curves show an acceptable quality, and therefore, the applicability of the model is justified. The diffusion coefficient *D* demonstrates a clear tendency to become larger with an increasing contribution from SAPC, which indicates an increasing (apparent) fluidity of the membrane bilayer at higher molar fractions of SAPC. The estimates for the global parameters are 3.1×10^{12} mol cm^{-2} for the concentration and 3720 cm s^{-1} for the intrinsic reaction rate. The latter observation indicates a finite (albeit rather high) reactivity of both reactants. In other words, there is a certain probability that the two reactants will not form an excimer upon contact.

Let us first compare the results of the analysis obtained earlier for the fluorescence decays of monomer and excimer emissions of $pyr_{10}PC$ in POPC.[7] Martins et al.[7] found at 35 °C $\tau_M = 206$ ns and $D = 5.5 \times 10^{-8}$ $cm^2\ s^{-1}$ for the analysis of monomer decay and $\tau_M = 196$ ns, $\tau_D = 58$ ns, and $D = 6.2 \times 10^{-8}$ $cm^2\ s^{-1}$ for the analysis of excimer emission. The monomer decay times are somewhat longer than those obtained in this work. The longer decay times found previously can be ascribed to removal of oxygen applied to the vesicle preparations, which was omitted in our preparations. The excimer decay times are in complete agreement. The diffusion coefficients of $pyr_{10}PC$ in POPC are significantly lower than those found in our study, even at the higher temperature of 35 °C. The reason for this may be found in the different parametrization used previously.[7] The approximation that the intrinsic reaction rate constant α approaches infinity—each bimolecular collision leads to excimer formation—was not taken into account in our model. To obtain an optimal fit, we had to include this parameter in the fitting procedure, and its finite value lends credence to the conclusion that some collisions do not give excimers. We also noticed that the

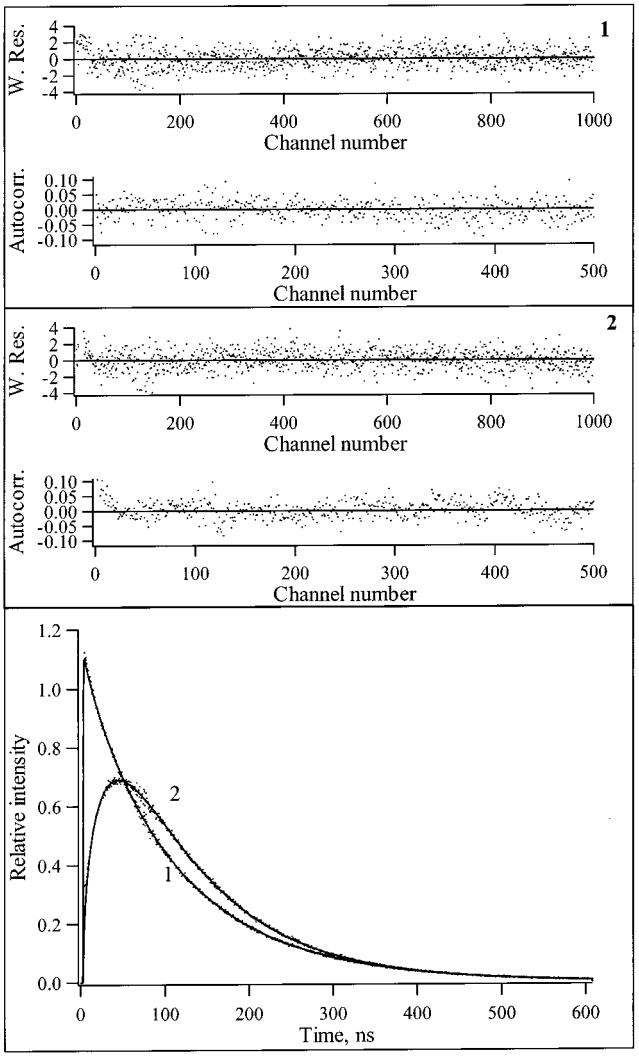

Figure 3. Reference reconvolution of the time dependence of the monomer (curve 1) and excimer (curve 2) fluorescence of $pyr_{10}PC$ in liposomes prepared from a mixture of DOPC and SAPC (molar ratio 1:1). The probe:phospholipid molar ratio was 1:150. The experimental curves are represented by points, and the fitted curves, by solid lines. The weighted residuals and autocorrelation of the residuals for both globally analyzed curves are randomly distributed around zero and are indicative of an optimal fit.

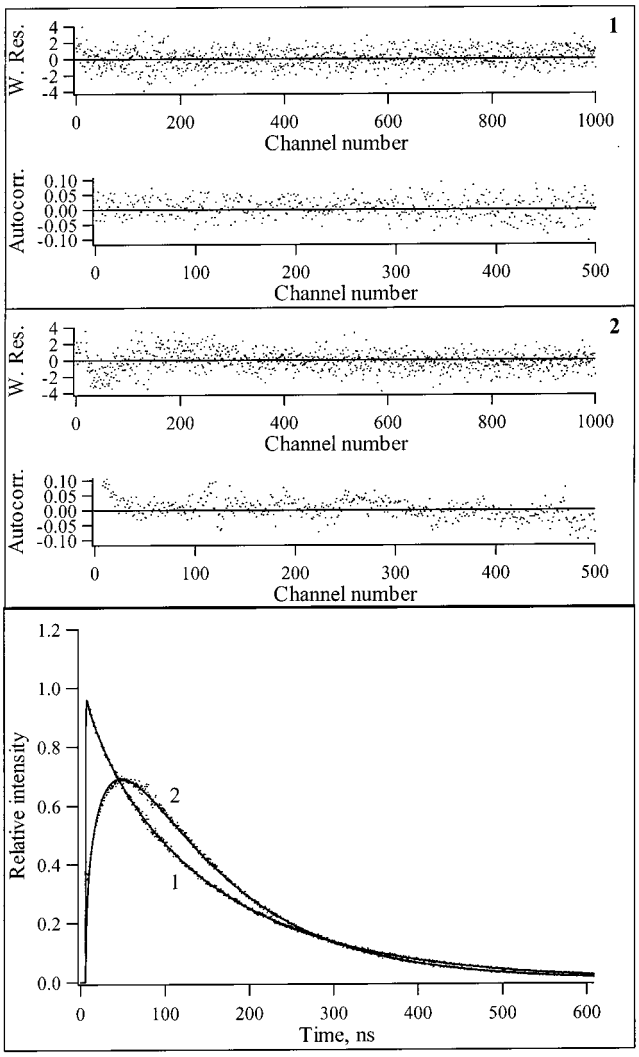

Figure 4. Reference reconvolution of the time dependence of the monomer (curve 1) and excimer (curve 2) fluorescence of $pyr_{10}PC$ in liposomes prepared from DPPC. The probe:phospholipid molar ratio was 1:150. The experimental curves are represented by points, and the fitted curves, by solid lines. The weighted residuals and autocorrelation of the residuals for both globally analyzed curves are randomly distributed around zero only for the monomer decay. The fit to the excimer emission was not optimal.

fitting parameters (D, α, and c) are highly correlated: any change in the optimal value of one of them will give different optimized values for the others. The advantage of global analysis linking common parameters over several experimental decays is obvious: the recovered parameters are better defined and the error estimates are significantly reduced.

The observation from both photostationary and time-resolved fluorescence experiments that a higher level of unsaturation in one of the chains (the case of SAPC) leads to more rapid lateral diffusion of $pyr_{10}PC$ is perhaps somewhat surprising (see Tables 1 and 2). It can also been seen that, next to the E/M values, D gradually increases with an increasing fractional concentration of SAPC. This indicates that the lipids are homogeneously dispersed in the SUV's and that $pyr_{10}PC$ does not show any preference for either DOPC or SAPC. In this respect, it is interesting to compare the lateral diffusion results with results obtained recently from measurements of the rotational mobilities of the membrane probe 1,6-diphenyl-1,3,5-hexatriene (DPH) dispersed in membrane bilayers consisting of highly polyunsaturated phospholipids.[24] Mitchell and Litman[24] found significantly slower rotational dynamics for DPH in DOPC than for DPH dispersed in 1-palmitoyl-2-arachidonyl-*sn*-glycero-3-phosphocholine (PAPC), which has a molecular structure comparable to that of SAPC. This is expressed in different rotational diffusion coefficients of the symmetry axis of DPH ($D_\perp$): at 20 °C, $D_\perp = 0.096$ ns^{-1} for DPH in DOPC and $D_\perp = 0.135$ ns^{-1} for DPH in PAPC. Of course, the rotational dynamics of the probe in the local lipid environment is measured, but these results are in complete agreement with the increased fluidity as obtained from the lateral diffusion measurements described in this work.

All attempts to combine the experimental time-dependent emission profiles obtained from $pyr_{10}PC$ in DPPC membranes into a single linkage scheme involving the results obtained with the unsaturated SUV's have failed. The estimated parameters are clearly different from those obtained from the time-resolved fluorescence of $pyr_{10}PC$

(24) Mitchell, D. C.; Litman, B. J. *Biophys. J.* **1998**, *74*, 879−891.

in the other unsaturated membranes. We have obtained an infinitely large value of the intrinsic reaction rate constant and a much higher value of the concentration (2.9×10^{13} mol cm^{-2}) along with a very low diffusion coefficient (0.46×10^{-8} cm^2 s^{-1}). Other parameters are $\tau_M = 210$ ns and $\tau_E = 69$ ns. Experimental and fitted curves are presented in Figure 4. SUV's composed of DPPC are rigid membranes at room temperature, and it is not surprising that the decay analysis failed to proceed correctly. The reason is that the excimer formation is diffusion controlled only above the phase transition temperature of the membrane.[2] In a strict sense, the kinetic model for a bimolecular reaction in a two-dimensional surface cannot be applied to analyze the fluorescence decay data of $pyr_{10}PC$ in membranes existing in the gel phase. However, from the parameter values recovered from the fitted decays (see Figure 4), one can arrive at an important qualitative conclusion. The effective concentration *c* is an order of magnitude larger than that found in fluid membranes, and the intrinsic reaction rate parameter α is infinitely large. This may indicate that $pyr_{10}PC$ forms molecular clusters (or domains) inside DPPC membranes stabilized by the weak dispersion forces of the pyrene aromatic rings. From geometric considerations, it was established previously that pyrene molecules located either in the same leaflet or in opposite leaflets can interact.[7]

Concluding Remarks

Global analysis of time-resolved pyrene monomer and excimer fluorescence using the model of reaction of two pyrene molecules in a two-dimensional lattice provides useful information on the lateral diffusion rate of the probe lipid. The large advantage of the time-resolved method over the photostationary method of measuring E/M ratios is that a single concentration of probe lipid can be used, whereas, for E/M measurements, the [probe]:[phospholipid] concentration ratio must be varied to recover the lateral diffusion coefficient.[2] Using the time-resolved fluorescence approach, however, one must carefully set up a linkage scheme for the global analysis, thereby linking common parameters such as concentration and intrinsic reaction rate constant. The procedure works very well in a comparative sense, for instance when membrane preparations with slightly altered properties are studied. For instance, in future work it will be of interest to systematically investigate the effect of cholesterol addition to liposomes on the lateral diffusion rate of the inserted pyrene phospholipid. Alternatively, one can think of addition of charged (unlabeled) phospholipids, pyrene phospholipids having a negatively charged headgroup, or membrane proteins to the membrane system to study the effects of repulsion or the presence of protein barriers on the phospholipid diffusion.[9]

A cautious remark should be made regarding the limitations of the model. Liposomes (especially SUV's) do not always form ideal planar surfaces. Long-range diffusion is supposed to take place over several micrometers,[7] and this distance rather corresponds to a curved area for small liposomes. For smaller aggregates such as micelles, the surface even resembles that of a sphere. In other words, the kinetic model has to be adapted for reactions taking place on a spherical surface instead of in a planar surface.[25,26] Not only longe-range diffusion but also diffusion over short distances (on the order of 10 nm or a few lipid molecules) can take place. This will be a factor to consider when the [probe]:[phospholipid] concentration ratio is relatively high (>1:100) and will lead to a discrepancy in the recovered diffusion coefficients. On the other hand, the short-range diffusion can be measured for dipyrenylphosphatidylcholine—which forms an intramolecular excimer—as a local membrane fluidity probe,[27−29] giving information similar to that yielded by the rotational diffusion probe DPH[23] or the phospholipid variant of DPH.[30,31] These experiments and global analyses are in progress in our laboratories.

Acknowledgment. This work was supported by EC-FAIR Project No. 97-3228.

LA000512R

(25) Adam, G.; Delbrück, M. In *Structural Chemistry and Molecular Biology;* Rich, A., Davidson, N., Eds.; W. H. Freeman: San Francisco, CA, 1968.
(26) Bodunov, E. N.; Berberan-Santos, M. N.; Martinho, J. M. G. *Chem. Phys. Lett.* **1998**, *297*, 419−427.
(27) Vauhkonen, M.; Sassaroli, M.; Somerharju, P.; Eisinger, J. *Biophys. J.* **1990**, *57*, 291−300.
(28) Sassaroli, M.; Vauhkonen, M.; Somerharju, P.; Scarlata, S. *Biophys. J.* **1993**, *64*, 137−149.
(29) Cheng, K. H.; Somerharju, P. *Biophys. J.* **1996**, *70*, 2287−2298.
(30) Pap, E. H. W.; ter Horst, J. J.; van Hoek, A.; Visser, A. J. W. G. *Biophys. Chem.* **1994**, *48*, 337−351.
(31) Pap, E. H. W.; Ketelaars, M.; Borst, J. W.; van Hoek, A.; Visser, A. J. W. G. *Biophys. Chem.* **1996**, *58*, 255−266.